International Journal of Environmental Sciences
ISSN: 2229-7359
Vol. 11 No. 22s, 2025
https://theaspd.com/index.php

Synthesis and Characterization of Nucleoside Analogues Derived from Glycine and Evaluation of Their Antioxidant Activity

Nabaa Abdul-Rasool Mahmood[1], Hala Mohammed Ghareeb[1]
[1]Department of Chemistry, College of Science, University of Kirkuk, Kirkuk, 36001, Iraq.
[*]Corresponding Author: scc23004@uokirkuk.edu.iq

Abstract
The synthesis, description, and assessment of the antioxidant activity of new nucleoside analogues produced from glycine are the main objectives of this work. In order to create nucleoside analogues, a multi-step synthetic process was used, starting with the synthesis of Schiff bases from aromatic aldehydes and aniline, followed by cyclization with glycine, fructose protection and bromination, and finally glycosylation. Nuclear magnetic resonance (^1H and ^{13}C NMR), Fourier-transform infrared spectroscopy (FT-IR), and thin-layer chromatography (TLC) were used to describe and confirm the structures of the produced compounds. The DPPH (2,2-diphenyl-1-picrylhydrazyl) free radical scavenging experiment was used to evaluate the compounds' antioxidant capability at different doses (10–100 µg/mL). The antioxidant activity of compounds (10) and (11) was significant (up to 81.25%), compound (9) was moderate, and compounds (12–14) were weak at lower concentrations but more effective at higher concentrations. These results support the potential use of glycine-based nucleoside analogues in oxidative stress-related medicinal applications and demonstrate their promising antioxidant qualities.
Keywords: Glycine, Nucleoside analogues, Antioxidant activity, Protected sugar, Schiff base

1. INTRODUCTION

Nucleoside analogues are important in medicinal chemistry because they mirror natural nucleosides while inhibiting nucleic acid synthesis in infections and aberrant cells. They are altered in the sugar moiety, nucleobase, or both to prevent viral replication, cancer, and other illnesses. The FDA has approved over 30 nucleoside analogues for antiviral, anticancer, antibacterial, and antiparasitic medicines, with development beginning in the 1940s. Cytarabine, licensed in the 1960s, was a milestone in leukemia treatment [1].

As demonstrated by acyclovir, zidovudine, and NM107 for HCV, nucleoside analogues offer a variety of therapeutic applications and function as antiviral medicines by blocking viral polymerases and stopping replication. Azacitidine and decitabine are used to treat cancer by inhibiting cell proliferation and reactivating tumor-suppressor genes. Multi-target therapy approaches are made possible by their mechanistic variety, which includes altering epigenetics, preventing nucleotide metabolism, and interfering with DNA repair [2].

Complex modifications, such as 4′/5′-spirocyclopropanated uridine, are present in recent analogues to improve stability, bioavailability, and specificity. Phosphate derivatives and other prodrug methods improve cellular absorption, while new scaffolds lessen resistance and toxicity.

With ongoing research in the treatment of neurological, metabolic, and infectious disorders, hybrid analogues with multiple alterations are being investigated for oncology and antiviral applications, especially against coronaviruses and resistant strains [3].

Glycine, the simplest amino acid, is an essential building component in bioorganic synthesis and enzymatic pathways [4]. Its structural simplicity makes it suitable for use in heme biosynthesis, engineered microbial production, and the synthesis of bioactive compounds [5]. The reversible glycine cleavage system (GCS) is used to generate glycine, which is essential for one-carbon metabolism and serves as the foundation for sustained bioproduction [6]. Its changeable structure also enables the green production of N-substituted molecules with potential medicinal applications [7].

An imbalance between reactive species (ROS/RNS) and antioxidant defenses leads to oxidative stress, which damages proteins, lipids, and DNA and is a contributing factor to aging, cancer, diabetes, cardiovascular disease, and neurological illnesses [8-10]. In order to protect cellular health, antioxidants fight this by chelating metals, neutralizing free radicals, and controlling redox signaling [11]. Their ability to prevent oxidative damage, lower inflammation, and promote disease prevention, healthy aging, and immunological function makes them potentially medicinal [12].

Specialized derivatives known as glycine nucleoside analogues, in which glycine is incorporated into nucleoside structures, have unique biochemical and medicinal advantages [13]. They may increase activity or get beyond barriers while simulating natural nucleosides [14]. Interestingly, glycine-linked nucleoside-β-amino acids function as uncharged DNA mimics that attach to RNA and DNA in a sequence-specific manner, indicating potential for molecular detection and treatment [15]. Advanced methods such as biocatalysis and stereoselective N-glycosylation are used in their production, which reflects attempts to increase sustainability and efficiency [16]. By altering nucleic acid metabolism, these analogues are essential in antiviral and anticancer therapies [17]. Research is still being done to tackle resistance and broaden their application to infections and neurological illnesses [18].

In order to change biological activity, early nucleoside analogue synthesis concentrated on changing the sugar and nucleobase. In particular, it targeted the 2′- and 3′-hydroxyl groups to produce chain terminators that stop DNA polymerization. Usually, chemical techniques entail creating synthetic sugars and then stereoselectively N-glycosylating them, which is essential for biological activity [19]. Several synthetic pathways include sugar phosphorylation, palladium-catalyzed nucleobase functionalization, and linear and modular approaches. Selective ring formation and stereoselective glycosylation are key components in the synthesis of 1,3-oxathiolane nucleosides, which are known for their antiviral properties [20]. Additionally, pure enantiomers are obtained through enzymatic resolution, which enhances pharmacological characteristics. All things considered, synthesis has progressed from straightforward adjustments to sophisticated chemical and enzymatic methods that allow for exact stereochemical control and the creation of potent antiviral and anticancer medications.

Current nucleoside analogue research faces key challenges: inefficient and rate-limiting phosphorylation limits active metabolite formation; poor oral bioavailability and cellular uptake hinder effective delivery [21]; unclear antibacterial mechanisms restrict repurposing [22]; few in vivo studies and clinical trials slow new applications [23]; resistance and toxicity are underexplored; synthesis methods are costly, slow, and limited in modification diversity[25]; and purification remains inefficient and environmentally challenging. These gaps hamper drug development and therapeutic optimization [25].

This work aims to synthesis and analyzes new glycine-derived nucleoside analogues and assess their antioxidant potential. The goal of the study is to investigate novel structural variations with possible metabolic benefits by adding glycine to the nucleoside framework. In order to help develop compounds with potential therapeutic uses in disorders linked to oxidative stress, the research aims to evaluate their structural integrity using spectroscopic methods and look into their capacity to scavenge free radicals.

2. MATERIALS AND METHODS

2.1. Materials

All materials were purchased from Merck® and used without further purification.

2.2. Procedures

2.2.1. Schiff Base Synthesis

An equimolar mixture (0.01 mol) of one of the aromatic aldehydes (p-hydroxybenzaldehyde, p-bromobenzaldehyde, or p-chlorobenzaldehyde), dissolved in 10 mL of absolute ethanol, was combined with aniline (0.01 mol) in a 150 mL round-bottom flask. A few drops of glacial acetic acid were added, and the reaction mixture was refluxed with continuous stirring for 12 hours at a temperature of 70–80 °C. Upon completion, the reaction mixture was allowed to cool, resulting in the formation of a precipitate. The solid product was then filtered, washed, and recrystallized from absolute ethanol, as illustrated in the equation below. Products formation **(1, 2, and 3)** was confirmed by thin-layer chromatography (TLC) using a mixture of (hexane: ethyl acetate) solvent system in a (7:3, v/v) ratio [26].

2.2.2. Cyclization Procedure

A total of 0.01 mol of Schiff bases **(1, 2,** and **3)** were dissolved in 15 mL of tetrahydrofuran (THF), followed by the addition of (0.01 mol) of glycine to the solution. The mixture was then refluxed for 48 hours. Upon completion of the reflux, the reaction mixture was cooled, and the resulting precipitate was collected and recrystallized using absolute ethanol. The progress and completion of the reaction were monitored by thin-layer chromatography (TLC) using a methanol–benzene solvent system in a **(4:1, v/v)** ratio, respectively. Affording compounds **(4, 5, and 6)** as pure products [27].

^{1}H NMR for **Compound (4)** (250 MHz, $CDCl_3$) δ (ppm): 3.73 (q, 2H), 6.81 (s, 1H), 7.20 (m, 1H), 7.22 (m, 1H), 7.35 (m, 1H), 7.36 (m, 1H), 8.58 (s, 1H). ^{13}C NMR (250 MHz, CDCl3) δ (ppm): 171.73, 157.86, 137.41, 132.83, 129.60, 126.28, 124.20, 114.80, 78.55, and 52.54.

^{1}H NMR for **Compound (5)** (250 MHz, $CDCl_3$) δ (ppm): 3.70 (q, 2H), 6.79 (s, 1H), 7.22 (m, 1H), 7.32 (m, 1H), 7.35 (s, 1H), 7.42 (m, 1H), 7.48 (m, 1H). ^{13}C NMR (250 MHz, CDCl3) δ (ppm): 171.73, 37.73, 130.89, 129.71, 126.27, 124.19, 122.60, 78.57, and 52.54.
^{1}H NMR for **Compound (6)** (250 MHz, $CDCl_3$) δ (ppm): 2.11 (m, 115H), 4.49 (dd, 2H), 4.84 (dd, 2H), 5.38 (d, 1H), and 5.32 (t, 1H). ^{13}C NMR (250 MHz, CDCl3) δ (ppm): 171.69, 149.09, 136.51, 135.35, 131.59, 129.71, 129.45, 129.09, 126.69, 81.03 and 51.51.

2.2.3. Fructose Protection Procedure

acetic anhydride (6 mL) was used to dissolve (1 g) of fructose (0.006 mol) and (0.8 g) of anhydrous sodium acetate (0.0097 mol). After that, the reaction mixture was heated for three hours while being constantly stirred in a water bath. After the acetylation was finished, the reaction product was extracted with chloroform and the solvent was evaporated to produce dark syrup. Using a (chloroform: methanol) solvent solution (4:1, v/v), thin-layer chromatography (TLC) was used to track the reaction and the formation of α-D-Fructofuranoside Pentaacetate (**Compound 7**) [28].
^{1}H NMR for **Compound (7)** (250 MHz, $CDCl_3$) δ (ppm): 3.92 (q, 2H), 6.80 (s, 1H), 7.26 (m, 1H), 7.41 (m, 1H), and 8.22 (s, 1H). ^{13}C NMR (250 MHz, CDCl3) δ (ppm): 170.81, 169.90, 107.75, 77.43, 75.40, 73.57, 64.95, 64.48, 21.44, 20.97, 20.87, 20.76 and 20.71.

2.2.4. General Procedure for the Preparation of 2-Bromo Acetyl Sugar N8

At 5°C, 3 mL of 50% hydrogen bromide in glacial acetic acid was added dropwise to dissolve the acetylated sugar N7 (0.006 mol). After an hour at 5 °C, the solution was transferred into 35 mL of chloroform and left to stand for 15 minutes at room temperature. To neutralize any residual acid, the mixture was next rinsed with ice-cold water (2 × 15 mL) and then saturated aqueous sodium bicarbonate solution. After a final wash with 20 milliliters of ice-cold water, the organic layer was dried on top of anhydrous magnesium sulfate ($MgSO_4$). **Compound 8** was obtained as an oily material by evaporating the solvent. TLC was used to track the reaction's progress (chloroform: methanol) (4:1) (v/v) ratio. Analogs of nucleosides were synthesized directly from the isolated bromo sugar [29].
1H NMR for **Compound (9)** (250 MHz, CDCl3) δ (ppm): 2.06 (m, 12H), 4.36 (q, 2H), 4.78 (q, 1H), 4.84 (dd, 2H), 5.30 (t, 1H), and 5.56 (d, 1H). ^{13}C NMR (250 MHz, CDCl3) δ (ppm):170.66, 170.61, 170.47, 169.99, 92.63, 77.54, 76.38, 74.10, 67.39, 64.43, 21.08, 20.88, 20.70, and 20.71.

2.2.5. Synthesis of Protected Nucleoside Analogs Derivatives (9, 10, 11)

After dissolving one of the compounds **(4, 5, and 6)** in (25 mL) of dry o-xylene, acetylated sugar bromide (0.001 mol) was added to the mixture. For an hour, the mixture was agitated. Anhydrous sodium sulfate was used to dry the organic layer after it had been cleaned with two milliliters of water. The acetylated nucleosides were then extracted by evaporating the solvent. Thin Layer Chromatography (TLC), employing a chloroform–methanol solvent combination in a 4:1 ratio, was used to track the reaction's development and conclusion [30].
^{1}H NMR for **Compound (9)** (250 MHz, $CDCl_3$) δ (ppm): 2.08 (q, 12H), 3.91 (q, 2H), 4.62 (m, 2H), 5.66 (m, 1H), 6.05 (s, 1H), 6.76 (m, 1H), 7.16 (m, 1H), and 8.58 (s, 1H). ^{13}C NMR (250 MHz, CDCl3) δ (ppm): 170.50, 157.41, 143.15, 132.58, 132.30, 129.12, 128.88, 126.08, 116.31, 109.35, 80.28, 65.13, 46.24, and 21.35.
^{1}H NMR for **Compound (10)** (250 MHz, $CDCl_3$) δ (ppm): 2.06 (q, 12H), 3.70 (q, 2H), 4.64 (m, 2H), 5.30 (m 1H), 6.05 (s, 1H), 7.39 (m, 1H), and 7.33 (m, 1H). ^{13}C NMR (250 MHz, CDCl3) δ (ppm): 173.25, 145.07, 142.11, 135.60, 132.79, 129.71, 129.17, 127.06, 121.52, 102.36, 77.64, 66.34, 53.04, and 18.91.
^{1}H NMR for **Compound (11)** (250 MHz, $CDCl_3$) δ (ppm): 2.04 (q, 12H), 3.70 (q, 2H), 4.76 (m, 2H), 5.30 (m 1H), 6.05 (s, 1H), 7.51 (m, 1H), and 7.33 (m, 1H). ^{13}C NMR (250 MHz, CDCl3) δ (ppm): 171.14, 170.49, 138.82, 134.94, 130.47, 129.06, 126.26, 124.38, 97.33, 80.10, 78.01, 74.94, 74.12, 65.11, 63.76, 53.39, and 20.90.

2.2.6. Hydrolysis for Protected Nucleosides Analog Derivatives (12, 13, 14)

Seven milliliters of 0.1 M sodium methoxide were used to heat a solution containing 0.003 mol of the protected nucleoside analogs **(9, 10, 11)** while stirring for half an hour. After neutralizing the reaction mixture with acetic acid, it was dried by evaporation. The residue was separated into water and chloroform, and the nucleoside analogs were obtained by vacuum-evaporating the aqueous layer until it was completely dry. TLC used a chloroform–methanol (4:1) solvent(v/v) ratio solution to track the reaction's progress and conclusion [31].
^{1}H NMR for **Compound (12)** (250 MHz, $CDCl_3$) δ (ppm): 3.78 (q, 2H), 3.94 (m, 1H), 4.00 (m, 2H), 4.53 (m, 1H), 6.00 (s, 1H), 7.31 (m, 1H), 7.38 (m, 1H), and 8.58 (s, 1H). ^{13}C NMR (250 MHz, CDCl3) δ

(ppm): 171.05, 139.08, 133.54, 130.41, 129.61, 126.26, 124.39, 115.84, 97.43, 84.11, 80.99, 76.70, 65.22, 63.10, 61.64, and 53.54.

^{1}H NMR for **Compound (13)** (250 MHz, $CDCl_3$) δ (ppm): 3.56 (q, 2H), 3.92 (m, 1H), 4.18 (m, 2H), 4.53 (m, 1H), 5.98 (s, 1H), 7.42 (m, 1H), and 7.33 (m, 1H). ^{13}C NMR (250 MHz, CDCl3) δ (ppm): 171.05, 138.73, 131.78, 130.48, 129.61, 126.26, 124.39, 122.60, 97.43, 84.11, 80.97, 76.70, 65.22, 61.64 and 53.54.

^{1}H NMR for **Compound (14)** (250 MHz, $CDCl_3$) δ (ppm): 3.77 (q, 2H), 3.99 (m, 1H), 4.03 (m, 2H), 4.53 (m, 1H), 6.01 (s, 1H), 7.40 (m, 1H), and 7.33 (m, 1H). ^{13}C NMR (250 MHz, CDCl3) δ (ppm): 172.50, 139.86, 135.30, 131.65, 130.29, 129.43, 128.57, 125.65, 100.97, 86.41, 69.35, 62.22, 25.32, and 30.85.

3. RESULTS AND DISCUSSIONS

3.1. Characterization of the Synthesized Compounds

This research covers the synthesis of many nucleoside analogues generated from certain amino acids. The compounds were characterized using TLC, FT-IR, NMR, and melting point determination, as reported in Chapter Two. The chemicals were produced using the experimental methodologies described in Chapter Two using the following scheme:

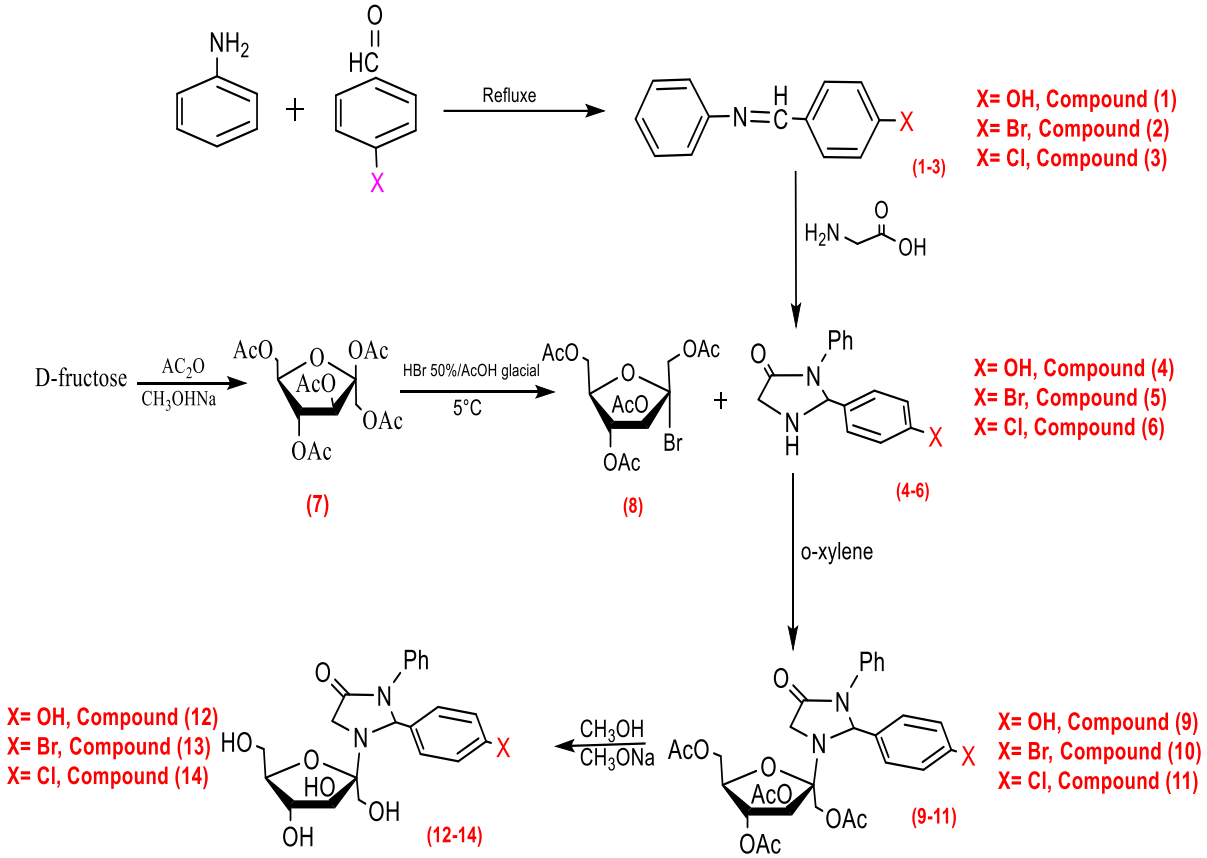

Scheme 1: Synthetic route of the prepared **compounds (1-14)**.

By monitoring changes in physical characteristics like color, melting point, and thin-layer chromatography (TLC), the reaction's occurrence was verified. FT-IR spectroscopy was used to analyze **Compounds 1, 2, and 3**. The C=O stretching band at 1687 cm^{-1} that was initially present in the reactant p-bromobenzaldehyde vanished, and an absorption band at 1621 cm^{-1} that corresponded to the stretching vibration of the C=N bond also emerged. The stretching vibration of the aliphatic C-H bonds that were created was also responsible for the absorption band at 2875 cm^{-1}, and the stretching vibration of the aromatic C-H bonds was responsible for the band at 3062 cm^{-1}. A distinct absorption band for the C-Br group was found at 539 cm^{-1}. Furthermore, absorption bands at 1584 cm^{-1} were ascribed to aromatic C=C stretching vibrations.

Compounds 4, 5, and 6 were also studied using FT-IR spectroscopy. The IR spectrum revealed two absorption bands: one at 2875 cm^{-1} for aliphatic (-CH_2-) stretching vibrations and another at 3100 cm^{-1} for aromatic (C-H) stretching vibrations. The N-H stretching was found at 3176 cm^{-1}, while the aromatic C=C stretching vibrations were attributed to 1588 cm^{-1}. At 1682 cm^{-1}, a significant absorption band developed, corresponding to the carbonyl group. The elimination of the absorption band at 1620 cm^{-1},

caused by the C=N stretching vibration, was detected. The C-Cl group attached to the benzene ring exhibited a distinct absorption band at 616 cm^{-1}. These findings are in good agreement with the literature [32].

Changes in the following compound's physical characteristics, including color, melting points, and thin-layer chromatography (TLC), were used to characterize it. FT-IR spectroscopy was also used to characterize **Compound 7**. The aliphatic (-CH_2-) stretching vibrations were identified by the IR spectra as the source of an absorption band at 2982 cm^{-1}, while the hydroxyl (-OH) group was responsible for the absorption band's disappearance at 3409 cm^{-1}. The carbonyl (C=O) group exhibited a significant absorption band at 1740 cm^{-1}, whereas the C–O stretching was represented by a band at 1216 cm^{-1}. Additionally, an absorption band attributed to the ether (C–O–C) group was detected at 1044 cm^{-1}.

Changes in physical characteristics, including color, melting points, and thin-layer chromatography (TLC), were used to characterize compound 8. Using FT-IR spectroscopy, the structure of **Compound 8** was confirmed. The stretching vibrations of aliphatic -CH_2- groups were represented by an absorption band in the infrared spectrum at 2929 cm^{-1}. The carbonyl (C=O) group was identified as the source of a strong absorption band at 1733 cm^{-1}, whereas the C–O stretching vibration was identified as the source of a band at 1220 cm^{-1}. The C–O–C functional group was identified by another absorption band at 1043 cm^{-1}, while the presence of a C–Br bond was revealed by a band at 603 cm^{-1}. Every finding agreed with the data from the literature [33].

Compound 9, 10, and 11 structures have been confirmed via using FT-IR spectroscopy. The stretching vibrations of aliphatic -CH_2- groups were represented by an absorption band at 2980 cm^{-1} in the infrared spectrum, whereas the aromatic C-H stretching vibrations were identified by another band at 3110 cm^{-1}. The C–O stretching was represented by an absorption band that emerged at 1222 cm^{-1}. The lack of the N–H bond was demonstrated by the elimination of the absorption band at 3176 cm^{-1}, which was previously ascribed to N–H stretching. Aromatic C=C stretching vibrations were identified as the source of a noticeable band at 1588 cm^{-1}. Furthermore, the presence of a carbonyl (C=O) group was confirmed by the appearance of a prominent absorption band at 1742 cm^{-1}. Additionally, the spectrum showed an absorption band at 693 cm^{-1}, which is the location of the C–Cl bond that is joined to a benzene ring. Every spectral data point agreed with the references in the literature [33].

As for **Compounds 12, 13, and 14**, the stretching vibrations of aliphatic -CH_2- groups were represented by an absorption band at 2926 cm^{-1} in the infrared spectrum, while aromatic C-H stretching vibrations were identified by a band at 3013 cm^{-1}. C–O stretching was identified by an absorption band at 1242 cm^{-1}, whereas the aromatic C=C stretching vibrations were identified by a band at 1557 cm^{-1}. A clear absorption band that showed the existence of a carbonyl (C=O) group also emerged at 1729 cm^{-1}. The 3200–3400 cm^{-1} range showed a large absorption band, which is indicative of hydroxyl (O–H) stretching. Every spectral data point agreed with the references in the literature [32,34].

3.2. Antioxidant Activity of the Synthesized Compounds

The antioxidant potential of selected synthesized compounds was evaluated using the stable DPPH (2,2-diphenyl-1-picrylhydrazyl) free radical scavenging assay to determine their antioxidant efficacy. Each compound was tested at concentrations of 10, 20, 40, 80, and 100 µg/mL. Absorbance was measured at a wavelength of 517 nm. Ascorbic acid was used as a standard antioxidant for comparison.

The antioxidant activity exhibited a positive correlation at higher concentrations, indicated by lower absorbance values. Active compounds were identified by a visible color change from the purple color of the DPPH reagent (violet control) to either colorless or yellowish hues. In contrast, inactive compounds retained the original violet color of the reagent.

Based on the graphical in **(Tables 1 and 2)** and **Figure (1)**, **compounds (10) and (11)** demonstrated high antioxidant activity, with **compound (10)** showing activity ranging from 65% to 78.75%, and **compound (11)** ranging from 71.25% to 81.25%. **Compound (9)** exhibited moderate activity, with percentages ranging from 37.5% to 53.75%. **Compounds (12), (13), and (14)** displayed weak activity at lower concentrations, but their antioxidant activity increased relatively at higher concentrations, reaching up to 75%.

The antioxidant activity of the produced nucleoside analogues of fructose with glycine derivatives varied depending on the molecule. **Compounds (10 and 11)** showed significant antioxidant activity, ranging from 65% to 81.25%, whereas **compound (9)** showed moderate activity, ranging from 37.5% to 53.75%. **Compounds (12, 13, and 14)** had modest antioxidant activities at low concentrations but improved significantly at higher concentrations, reaching up to 75%. These data show intriguing similarities and

differences when compared to findings from other investigations. Using the DPPH assay, for instance, Ficus religiosa extract demonstrated 43.415% activity, which is comparable to **compound (9)**, but lower than **compounds (10 and 11)**. **Compounds (10) and (11)** outperformed glutathione (GSH) and its analogues in terms of DPPH percentage [35], while **compounds (12 to 14)** were comparable to weaker amino acids like taurine, which exhibited little to no activity. L-cysteine had the highest activity in studies of amino acid derivatives [36]. Cytidine tetracaffeate [37], a nucleoside conjugate, had noticeably more antioxidant effects than caffeic acid alone in the field of nucleoside-based antioxidants, mirroring the increased activity shown in **compounds (10 and 11).** The notion that structural alteration via nucleoside conjugation, especially with glycine derivatives, is a promising strategy to increase antioxidant capacity is supported by these studies. Furthermore, research on amino acids have shown that higher concentrations enhance radical scavenging activity, which is consistent with the concentration-dependent behavior shown in weaker **compounds (12–14)** [38-40].

Table 1. Results of the Percentage Radical Scavenging Activity (%RSA) Test to Determine the Antioxidant Efficacy of **Compounds (9, 10, 11, 12, 13, 14)** Using the DPPH Reagent.

Compounds	Produced compounds' percentage of free radical scavenging activity (RSA%) at different concentrations (µg/mL)				
	10%	20%	40%`	80%	100%
9	37.5	42.5	43.75	50	53.75
10	65	68.75	75	77.5	78.75
11	71.25	72.75	75	77.5	81.25
12	0	0	0	50	75
13	0	62.5	65	75	75
14	0	0	0	52.5	75
Ascorbic Acid	12.5	37.5	72.5	73.75	76.25

Table 2. Absorbance Values in the Antioxidant Activity Assay for the Synthesized **Compounds (9, 10, 11, 12, 13, 14)** Using the DPPH Reagent.

Compounds	Absorbance (Abs) Values of the Synthesized Compounds at Different Concentrations Measured at a Wavelength of 517 nm				
	10%	20%	40%`	80%	100%
9	0.5	0.46	0.45	0.4	0.37
10	0.28	0.25	0.20	0.18	0.17
11	0.23	0.218	0.2	0.18	0.15
12	0.8	0.8	0.8	0.4	0.2
13	0.8	0.3	0.28	0.2	0.2
14	0.8	0.8	0.8	0.38	0.2
Ascorbic Acid	0.7	0.5	0.22	0.21	0.19
DPPH	0.8	0.8	0.8	0.8	0.8

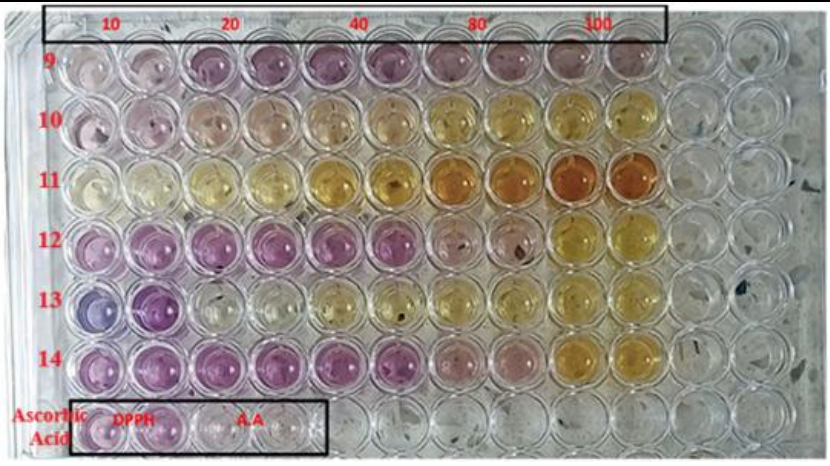

Fig. 1. Antioxidant Activity Test Results of the Compounds (9, 10, 11, 12, 13, 14, and ascorbic acid).

4. CONCLUSIONS

In this work, glycine-derived nucleoside analogues were successfully synthesized, characterized, and their antioxidant activity was assessed using the DPPH assay. **Compounds (10) and (11)** exhibited considerable

activity, while **compounds (9) and (12–14)** were moderately active at low concentrations but improved at higher ones. The outcomes reinforce the therapeutic promise of glycine-conjugated nucleoside analogues against disorders linked to oxidative stress by highlighting their potential as powerful antioxidants and correlating with earlier research.

REFERENCES

[1] Seley-radtke KL, Yates MK. Since January 2020 Elsevier has created a COVID-19 resource centre with free information in English and Mandarin on the novel coronavirus COVID- 19 . The COVID-19 resource centre is hosted on Elsevier Connect , the company ' s public news and information. Antiviral Res. 2018;154(January):66–86. https://doi.org/10.1016/j.antiviral.2018.04.004
[2] Wang P, Cheng T, Pan J. Nucleoside analogs: a review of its source and separation processes. Molecules. 2023;28(20):7043. https://doi.org/10.3390/molecules28207043.
[3] Al Awadh AA. Nucleotide and nucleoside-based drugs: Past, present, and future. Saudi J Biol Sci. 2022;29(12):103481. https://doi.org/10.1016/j.sjbs.2022.103481
[4] Yitzhaki M, Ben-Tamar D. Number of references in biochemistry and other fields; A case study of the Journal of Biological Chemistry throughout 1910-1985. Scientometrics. 1991;21(1):3–22. https://doi.org/10.1007/bf02019179
[5] Kosmopoulos C. From open access publishing to open science: An overview of the last developments in Europe and in France. Handb Res Glob View Open Access Sch Commun. 2022;1–22. https://doi.org/10.1073/pnas.2200413119
[6] Jafari A, Eslami Moghadam M, Mansouri-Torshizi H. Green synthesis and bioactivity of aliphatic N-substituted Glycine derivatives. ACS omega. 2023;8(33):30158–76. https://doi.org/10.1021/acsomega.3c02828
[7] Xu Y, Ren J, Wang W, Zeng A. Improvement of glycine biosynthesis from one-carbon compounds and ammonia catalyzed by the glycine cleavage system in vitro. Eng Life Sci. 2022;22(1):40–53. https://doi.org/10.1002/elsc.202100047
[8] Kotha RR, Tareq FS, Yildiz E, Luthria DL. Oxidative stress and antioxidants—A critical review on in vitro antioxidant assays. Antioxidants. 2022;11(12):2388.
[9] https://doi.org/10.3390/antiox11122388
[10] Tan BL, Norhaizan ME, Liew WPP, Sulaiman Rahman H. Antioxidant and oxidative stress: a mutual interplay in age-related diseases. Front Pharmacol. 2018; 9:1162. https://doi.org/10.3389/fphar.2018.01162
[11] Chaudhary P, Janmeda P, Docea AO, Yeskaliyeva B, Abdull Razis AF, Modu B, et al. Oxidative stress, free radicals and antioxidants: potential crosstalk in the pathophysiology of human diseases. Front Chem. 2023;11(May):1–24.https://doi.org/10.3389/fchem.2023.1158198
[12] Chandimali N, Bak SG, Park EH, Lim HJ, Won YS, Kim EK, et al. Free radicals and their impact on health and antioxidant defenses: a review. Cell Death Discov [Internet]. 2025;11(1). https://doi.org/10.1038/s41420-024-02278-8
[13] Pisoschi AM, Pop A, Iordache F, Stanca L, Predoi G, Serban AI. Oxidative stress mitigation by antioxidants-an overview on their chemistry and influences on health status. Eur J Med Chem. 2021;209:112891. https://doi.org/10.1016/j.ejmech.2020.112891
[14] Das A, Pradhan B. A facile route to synthesize N-(Boc-Aminoethylglycin) thymine Ethyl Ester, application to the synthesis of PNA-oligonucleotide conjugates. J Chem Sci [Internet]. 2020;132(1). https://doi.org/10.1007/s12039-020-1738-y
[15] Chen H, Lawler JL, Filman DJ, Hogle JM, Coen DM. Resistance to a nucleoside analog antiviral drug from more rapid extension of drug-containing primers. MBio. 2021;12(1):1–16.https://doi.org/10.1128/mbio.03492-20
[16] Tsesmetzis N, Paulin CBJ, Rudd SG, Herold N. Nucleobase and nucleoside analogues: Resistance and re-sensitisation at the level of pharmacokinetics, pharmacodynamics and metabolism. Cancers (Basel). 2018;10(7). https://doi.org/10.3390/cancers10070240
[17] Hruba L, Das V, Hajduch M, Dzubak P. Nucleoside-based anticancer drugs: Mechanism of action and drug resistance. Biochem Pharmacol [Internet]. 2023;215(August):115741. https://doi.org/10.1016/j.bcp.2023.115741
[18] Maria C, Rauter AP. Nucleoside analogues: N-glycosylation methodologies, synthesis of antiviral and antitumor drugs and potential against drug-resistant bacteria and Alzheimer's disease. Carbohydr Res. 2023; 532:108889. https://doi.org/10.1016/j.carres.2023.108889
[19] Salihovic A, Taladriz-Sender A, Burley GA. Preparation of nucleoside analogues: opportunities for innovation at the interface of synthetic chemistry and biocatalysis. Chem Sci. 2025; https://doi.org/10.1039/D5SC03026A
[20] Rando HM, Wellhausen N, Ghosh S, Lee AJ, Dattoli AA, et al. Identification and Development of Therapeutics for COVID-19. Vol. 6, mSystems. 2021. https://greenelab.github.io/covid19-review/
[21] Shaughnessy KH. Palladium-catalyzed modification of unprotected nucleosides, nucleotides, and oligonucleotides. Molecules. 2015;20(5):9419–54.
[22] https://doi.org/10.3390/molecules20059419
[23] Aher UP, Srivastava D, Singh GP, Jayashree BS. Synthetic strategies toward 1,3-oxathiolane nucleoside analogues. Beilstein J Org Chem. 2021; 17:2680–715. https://doi.org/10.3762/bjoc.17.182
[24] Thomson JM, Lamont IL. Nucleoside analogues as antibacterial agents. Front Microbiol. 2019; 10:952. https://doi.org/10.3389/fmicb.2019.00952
[25] Xu X, Li Z, Yao X, Sun N, Chang J. Advanced prodrug strategies in nucleoside analogues targeting the treatment of gastrointestinal malignancies. Front Cell Dev Biol. 2023;11(April):1–8. https://doi.org/10.3389/fcell.2023.1173432
[26] Ibraheem S, Al-Khazraji C, Mohammad H, Al-Zahawi G, Albayati MR. Synthesis, Characterization and Enzymetic Evaluation of Novel Bis Derivatives of Azetidinone and Oxazolidinone Derived From Orthotolidine. WORLD J Pharm Pharm Sci S JIF Impact Factor 6 [Internet]. 2016;041(11):193. https://doi.10.20959/wjpps201611-7
[27] Kamal R. Synthesis and identification of some new heterocyclic derivatives from carbonyl and carboxyl compounds and study of their biological activity [MSc thesis]. Al-Qadisiyah University; 2019.

[28] Al-Mouamin TM, Kadhim AK. Synthesis and Characterization of Some New Nucleoside Analogues from Substituted Benzimidazole via 1, 3-Dipolar cycloaddition. Baghdad Science Journal. 2016 Jun 5;13(2.2 NCC):0298-.
[29] AL-Zahawi H. Synthesis of a new fructo-nucleoside analogue derivatives and their inhibitory effect on alkaline phosphatase activity in breast cancer disease. Al-Mostansiriah; 1999.
[30] Al-Mouamin TM, Mehdi DJ. Synthesis of novel Nucleoside Analogues from Imidizoline and Evaluation their Anti microbial Activity. Iraqi Journal of Science. 2016;57(1A):14-27.
[31] Shiao TC, Giguère D, Wisse P, Roy R. 33 Synthesis of Phenyl. Carbohydrate Chemistry: Proven Synthetic Methods, Volume 2. 2014 Mar 4:269.
[32] Clerc JT. Computer methods for the spectroscopic identification of organic compounds. Pure Appl Chem. 1978;50(2):103–6. https://doi.org/10.1351/pac197850020103
[33] AL-Dawoody P, AL-Zahawi H, Chelebi N. Preparation and characterization of some pyrimidine derivatives and study with CT DNA. InAIP Conference Proceedings 2023 Sep 29 (Vol. 2839, No. 1). AIP Publishing.
[34] Silverstein RM, Bassler GC. Spectrometric identification of organic compounds. J Chem Educ. 1962;39(11):546. https://doi.org/10.1021/ed039p546
[35] Hussain H, Ahmad S, Shah SW, Ullah A, Almehmadi M, Abdulaziz O, Allahyani M, Alsaiari AA, Halawi M, Alamer E. Investigation of antistress and antidepressant activities of synthetic curcumin analogues: Behavioral and biomarker approach. Biomedicines. 2022 Sep 24;10(10):2385.
[36] Monteiro LS, Paiva-Martins F. Amino acids, amino acid derivatives and peptides as antioxidants. InLipid Oxidation in Food and Biological Systems: A Physical Chemistry Perspective 2022 Feb 6 (pp. 381-404). Cham: Springer International Publishing.
[37] Zhao PF, Liu ZQ. Equipping Uridine with Three Dipeptide Motifs for the Inhibition of Radical-Induced DNA Oxidation. The Journal of Organic Chemistry. 2024 Aug 29;89(18):13059-70.
[38] Tang Y, Debnath T, Choi EJ, Kim YW, Ryu JP, Jang S, Chung SU, Choi YJ, Kim EK. Changes in the amino acid profiles and free radical scavenging activities of Tenebrio molitor larvae following enzymatic hydrolysis. PLoS One. 2018 May 4;13(5):e0196218.
[39] Guidea A, Zăgrean-Tuza C, Moţ AC, Sârbu C. Comprehensive evaluation of radical scavenging, reducing power and chelating capacity of free proteinogenic amino acids using spectroscopic assays and multivariate exploratory techniques. Spectrochimica Acta Part A: Molecular and Biomolecular Spectroscopy. 2020 Jun 5;233:118158.
[40] Michail K, Baghdasarian A, Narwaley M, Aljuhani N, Siraki AG. Scavenging of free-radical metabolites of aniline xenobiotics and drugs by amino acid derivatives: toxicological implications of radical-transfer reactions. Chemical research in toxicology. 2013 Dec 16;26(12):1872-83.